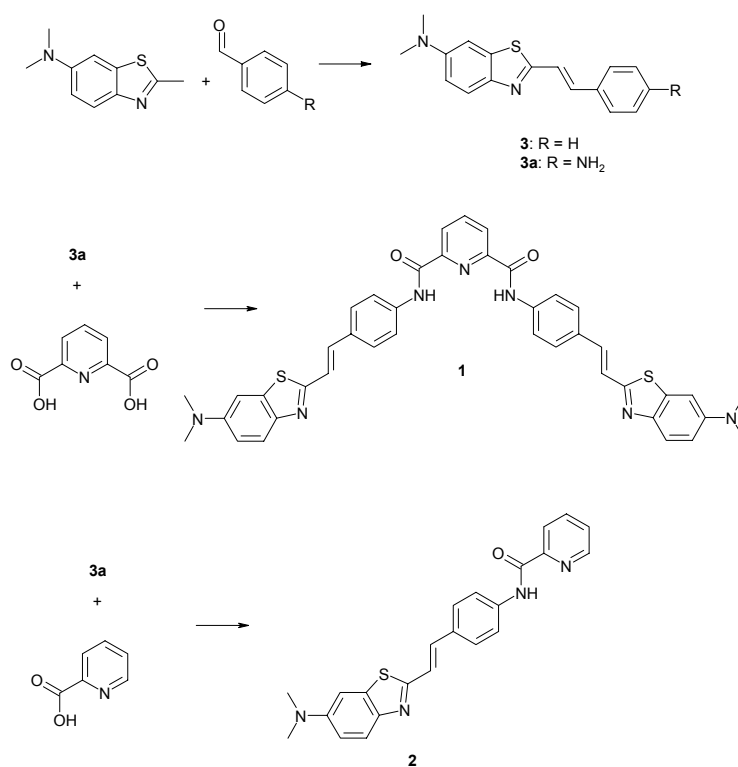# A charge transfer-type fluorescent molecular sensor that "lights up" in the visible upon hydrogen bond-assisted complexation of anions

Anton Kovalchuk, Julia L. Bricks, Günter Reck, Knut Rurack,* Burkhard Schulz, Agnieszka Szumna and Hardy Weißhoff

Electronic Supporting Information

S1. Synthesis.

Scheme S1. Synthetic route to **1–3** and **3a**.

Synthesis of *N,N*-dimethyl-2-[(E)-2-phenylvinyl]-1,3-benzothiazol-6-amine 3. A mixture of 0.576 g (3 mmol) 6-*N,N*-dimethylamino-2-methylbenzothiazole, 0.636 g (6 mmol) benzalde-hyde and 0.5 g powdered KOH was stirred for 5 h at 25°C in 5 mL DMF. After pouring the reaction mixture into 25 mL water, a solid was filtered off and washed with water. The crude product was purified by recrystallization from isopropanol (twice), yielding a yellow powder. Yield 0.625 g (74 %); m.p. 146–148°C. Elemental analysis, found: C, 72.68; H, 5.62; N, 10.04; calc. for $C_{17}H_{16}N_2S$: C, 72.82; H, 5.75; N, 9.99. ^{1}H NMR (CDCl$_3$) δ (ppm): 3.03 [BT–N(CH$_3$)$_2$, s, 6H], 6.95–6.92 (BT–H, d, 1H), 7.08 (BT–H, s, 1H), 7.33–7.32 (PhH, m, 1H), 7.37–7.34 (PhH, m, 2H), 7.40–7.37 and 7.39–7.36 (-CH=CH–, 2 × d, J = 14.7 Hz, 2H), 7.56–7.54 (PhH, d, 2H), 7.83–7.81 (BT–H, d, 1H).

Synthesis of 2-[(E)-2-(4-aminophenyl)vinyl]-1,3-benzothiazol-6-amine 3a. A mixture of 1.5 g (7.8 mmol) 6-*N,N*-dimethylamino-2-methylbenzothiazole, 1.18 g (7.8 mmol) 4-aminobenzaldehyde and 0.2 mL 30 % aqueous solution of tetramethylammonium hydroxide were reacted in 10 mL DMSO for 20 h at 70°C. After cooling, a precipitate was filtered off and

the remaining mixture was poured onto 25 mL ice. The solid was treated with isopropanol, filtered and washed again with isopropanol. The product was purified by recrystallization from isopropanol, yielding a yellow powder (1.397 g, yield 55 %). After melting point and NMR analysis, **3a** was directly used for the preparation of **1** and **2**. M.p. 208–210°C. ^{1}H NMR (DMSO) δ (ppm): 2.97 [BT–N(CH$_3$)$_2$, s, 6H], 6.90–6.99 (BT–H, d, 1H), 7.07 (BT–H, s, 1H), 7.25–7.22 and 7.23–7.21 (-CH=CH–, 2 × d, J = 14.8 Hz, 2H), 7.37–7.34 (PhH, m, 2H), 7.38–7.35 (PhH, d, 2H), 7.67–7.64 (BT–H, d, 1H).

Synthesis of *N*,*N*′-bis(4-{(E)-2-[6-(dimethylamino)-1,3-benzothiazol-2-yl]vinyl}phenyl)pyridine-2,6-dicarboxamide 1. A mixture of 0.815 g (2.8 mmol) **3a** and 0.238 g (1.4 mmol) pyridine-2,6-dicarboxylic acid was stirred for 10 min at 40°C in 5 mL pyridine. Then 0.85 g (2.8 mmol) triphenyl phosphite was added dropwise, and the reaction mixture was heated up to 90°C for 3.5 h. After cooling, the mixture was stirred overnight at room temperature. Addition of 10 mL water afforded a precipitate that was filtered off, washed with water and dried. The product was purified by recrystallization from 3 mL DMF and 0.793 g (yield: 78 %) orange crystals were obtained. M.p. 323–325°C. Elemental analysis, found: C, 67,72; H, 5.12; N, 14,05; calc. for C$_{41}$H$_{35}$N$_7$O$_2$S$_2$: C, 68.22; H, 4.89; N, 13.58. ^{1}H NMR (DMSO) δ (ppm): 3.00 [BT–N(CH$_3$)$_2$, s, 12H], 6.97–6.99 (BT–H, d, 2H), 7.29 (BT–H, s, 2H), 7.51–7.49 and 7.48–7.45 (-CH=CH–, 2 × d, J = 15.0 Hz, 4H), 7.76–7.73 (BT–H, d, 2H), 7.84–7.82 (PhH, d, 4H), 8.05–8.03 (PhH, d, 4H), 8.34 (Pyr–H, d, 1H), 8.44 (Pyr–H, d, 2H), 11.19 (NH, s, 2H).

Synthesis of *N*-(4-{(E)-2-[6-(dimethylamino)-1,3-benzothiazol-2-yl]vinyl}phenyl)pyridine-2-carboxamide 2. By analogy with **1**, a mixture of 0.408 g (1.4 mmol) **3a** and 0.238 g (1.4 mmol) pyridine-2-carboxylic acid was treated in a similar way and, after reaction with 0.42 g (1.4 mmol) triphenyl phosphite and subsequent treatment as above, yielded 0.386 g (yield: 69 %) of reddish orange crystals. M.p. 238–240°C. Elemental analysis, found: C, 68,32; H, 4,78; N, 14.52; calc. for C$_{23}$H$_{20}$N$_4$OS: C, 68.98; H, 5.03; N, 13.99. ^{1}H NMR (DMSO) δ (ppm): 3.00 [BT–N(CH$_3$)$_2$, s, 6H], 6.95–6.98 (BT–H, d, 1H), 7.28 (BT–H, s, 1H), 7.41–7.38 and 7.46–7.43 (-CH=CH–, 2 × d, J = 14.7 Hz, 2H), 7.70 (Pyr–H, m, 1H), 7.75–7.73 (PhH, d, 2H), 7.74–7.72 (BT–H, d, 1H), 8.02–8.00 (PhH, d, 2H), 8.09 (Pyr–H, t, 1H), 8.18 (Pyr–H, d, 1H), 8.77–8.75 (Pyr–H, d, 1H), 10.8 (NH, s, 1H).

S2. X-ray structure analysis. The X-ray data of the two solvates **1×DMF** and **1×DMSO** were collected on a Bruker SMART CCD and a KUMA CCD diffractometer, respectively. The structures were solved by direct methods and refined by full-matrix least-squares calculations using SHELXTL.[1] The hydrogen atoms were introduced in their calculated positions and refined using the riding model. In both structures, the DMF and DMSO molecules are occupationally disordered. The structure of **1×DMSO** contains additionally 2.5 THF molecules in the asymmetric unit, showing also an occupational disorder. For the structure determination of **1×DMSO**, only single crystals of very poor quality were available. Thus, restraints for bond lengths and displacement parameters were used in the structure refinement. The crystallographic data and details of the structure analysis of **1×DMF** and **1×DMSO** are collected in Table S1. CCDC-234956 (**1×DMF**) and CCDC-234957 (**1×DMSO**) contain the complete crystallographic data for this paper. These data can be obtained free of charge via www.ccdc.ac.uk/conts/retrieving.html (or from the Cambridge Crystallographic Data Centre, 12, Union Road, Cambridge CB21EZ, UK; deposit@ccdc.cam.ac.uk; or fax: (+44)1223-336-033).

S2.1. Molecular conformations. The molecular conformation of both compounds (Figure S1) can be described by root mean squares (r.m.s) deviations of the atoms from planes, dihedral angles, and torsion angles.

In **1×DMF** as well as **1×DMSO**, the right-hand part of the molecule is virtually planar. The r.m.s. deviatons of atoms N1, C2, C3, C4, C2', C3'…C27 amount to 0.079 and 0.082 Å. For the

second arm of the molecule (N1…C27'), r.m.s. values of 0.984 and 0.217 Å are found. The coplanarity of the right arm of the molecules is also indicated by the following dihedral angles, $\theta_{\text{rings 1–2}}$ = 4.62° and 6.90° for **1×DMF** and **1×DMSO**, respectively, as well as $\theta_{\text{rings 2–3/4}}$ = 6.32° and 8.93° and $\theta_{\text{rings 1–3/4}}$ = 4.89° and 4.92° (for the labeling of the rings, see Figure S1). The highly twisted form of the left arm of the molecule **1×DMF** is again reflected in the dihedral angles, amounting to $\theta_{\text{rings 1–2'}}$ = 24.94°, $\theta_{\text{rings 2'–3'/4'}}$ = 35.58° and $\theta_{\text{rings 1–3'/4'}}$ = 59.85°. The corresponding values are significantly smaller in **1×DMSO** (28.24°, 15.71° and 14.36°), indicating the more overall planar structure of this solvate. The main effects that cause the differences in conformation of the left arms of the two solvates are the torsion angles around the single bonds N6'–C8' and C11'–C14', C5'–N6'–C8'–C9' = 28.5° and –27.1° as well as C12'–C11'–C14'–C15' = 21.3° and –170.5°, respectively.

Despite these conformational differences, the overall shapes of **1×DMF** and **1×DMSO** are very similar as manifested in the distances Cg(1)---N25 = 17.65 and 17.61 Å, Cg(1)---N25' = 17.59 and 17.60 Å as well as N25---N25' = 24.39 and 24.09 Å, respectively, with Cg(1) being the centroid of the ring 1.

Table S1 Crystallographic data and details of the structure determination of **1×DMF** and **1×DMSO**

	1×DMF	**1×DMSO**
formula	$C_{41}H_{35}N_7O_2S_2$xDMF	$C_{41}H_{35}N_7O_2S_2$xDMSO.2.5THF
molecular weight	794.98	980.27
T[K]	298(2)	298(2)
crystal system	monoclinic	triclinic
space group	$P2_1/c$	P-1
a[Å]	8.549(2)	8.598(2)
b[Å]	31.823(6)	12.400(2)
c[Å]	14.972(3)	26.453(4)
α[°]	90	99.094(14)
β[°]	97.703(4)	97.226(14)
γ[°]	90	107.448(17)
V[Å³]	4036.3(12)	2611.3(8)
Z	4	2
$\rho_{\text{calc.}}$[gcm⁻³]	1.308	1.247
μ[mm⁻¹]	0.183	0.196
F(000)	1672	1040
crystal size [mm]	0.30 x 0.10 x 0.08	0.21 x 0.07 x 0.07
Θ_{max} [°]	25.0	23.0
index ranges	–12/10, –45/38, –15/19	–9/9, –13/13, –29/29
unique reflections	7108	7217
reflections observed [I>2σ(I)]	2567	1624
parameter / restraints	506 / 11	717 / 110
R1(on F) [I>2σ(I)]	0.053	0.112
wR2(on F²)	0.146	0.261
largest diff. peak/hole	0.43 / –0.26	0.60 / –0.41

S2.2. Hydrogen bonding. As shown in Figure S1, in **1×DMF** as well as in **1×DMSO** the solvent molecules are held by the sensor molecule **1** via two intermolecular hydrogen bonds N6–H…O and N6'–H…O (Table S2). Despite these bonds, however, the DMF as well as the DMSO molecule are positionally disordered, i.e. in both structures two positions for DMF and DMSO were found. In Figure S1, only one postion is shown for clarity. Besides the intermolecular bonds also intramolecular N-H…N hydrogen bonds exists in both crystal structures.

Table S2 Hydrogen bonds in **1×DMF** and **1×DMSO** ("D" and "A" denote the hydrogen bond donor and acceptor atoms, d are distances and α are angles)

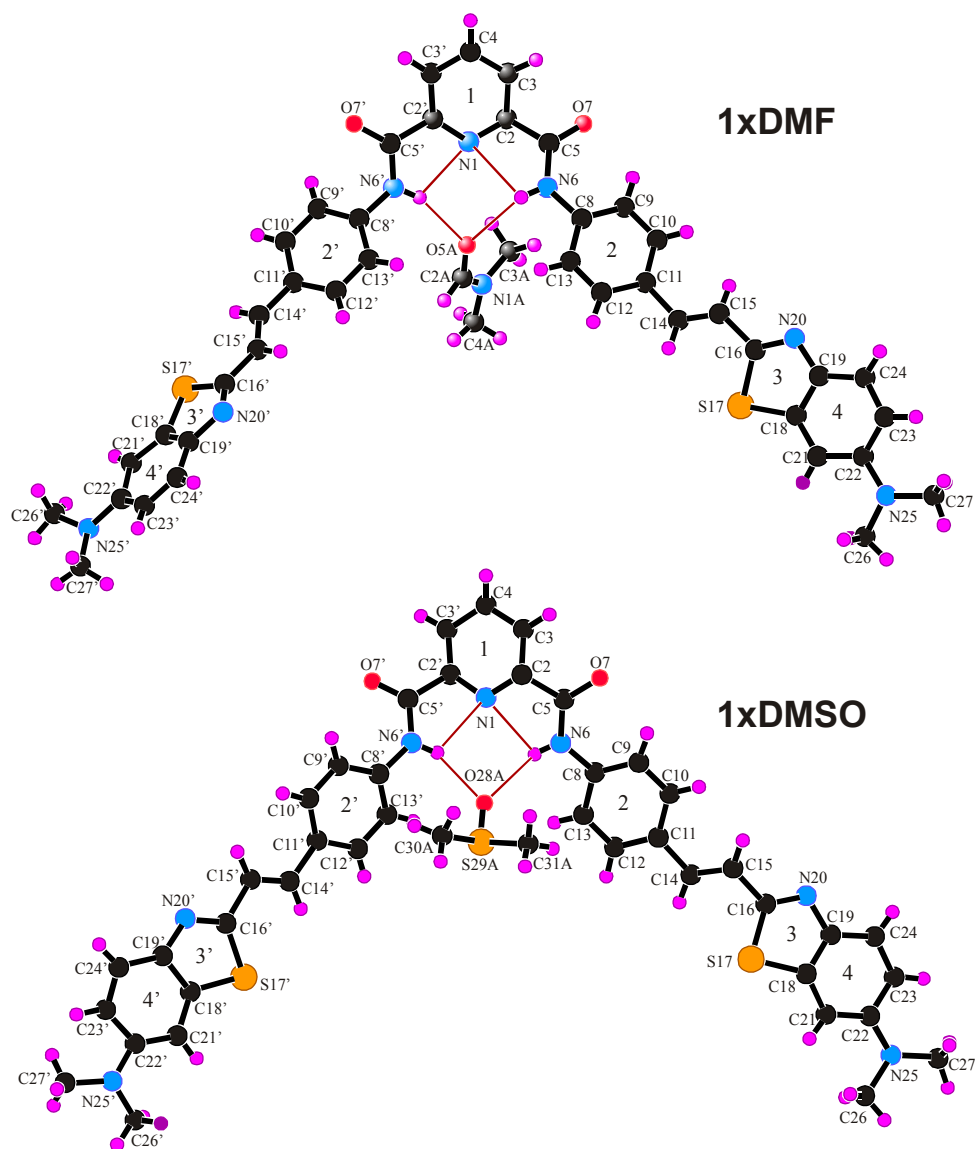| D–H…A	d(D–H) /Å	d(H...A) /Å	α(DHA) /deg.	d(D…A) /Å
1×DMF				
N6–H6...O5A	0.86	2.33	151.2	3.113
N6–H6...O5B	0.86	2.28	150.2	3.053
N6'–H6'...O5A	0.86	2.10	153.4	2.892
N6'–H6'...O5B	0.86	2.31	155.6	3.116
N6–H6…N1	0.86	2.32	110.2	2.736
N6'–H6'…N1	0.86	2.29	110.2	2.709
1×DMSO				
N6–H6...O28A	0.86	2.28	149.5	3.051
N6–H6...O28B	0.86	2.20	143.5	2.938
N6'–H6'...O28A	0.86	2.18	149.9	2.961
N6'–H6'...O28B	0.86	2.16	147.3	2.924
N6–H6…N1	0.86	2.29	107.6	2.670
N6'–H6'…N1	0.86	2.31	109.6	2.722

Figure S1 Crystal structures of the two solvates of **1**

S2.3. π–π Electron interactions. π–π Electronic interactions between neighboring molecules can be of importance for the stabilization of supramolecular structures in the solid-state, resulting in certain one-, two- or three-dimensional networks. They can also have an impact on spectroscopic properties of compounds in the crystalline state. These interactions are defined by the distance between the ring centroids (DC), the perpendicular distance of the centroid of one ring from the plane of the other (DP) and the interplanar angle α. The parameters collected in Table S3 were derived from the two crystal structures.
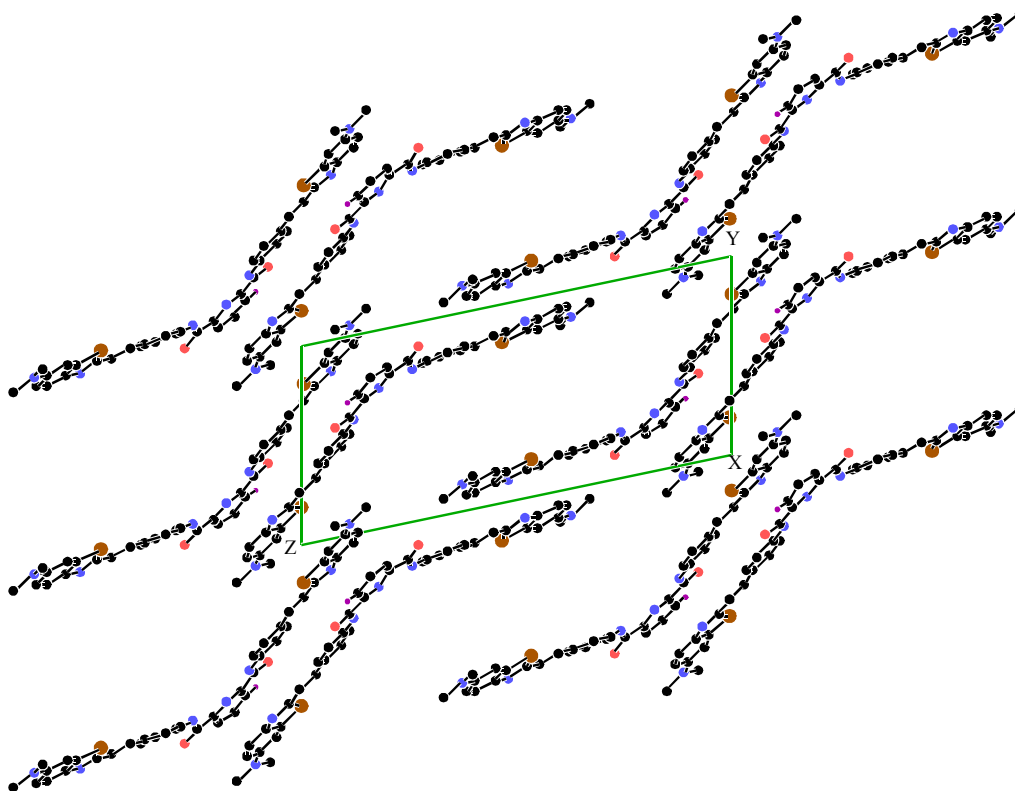

Figure S2 Molecular layers in the crystal structure of **1×DMSO**, solvent molecules and hydrogen atoms were omitted for clarity

Table S3 Parameters governing the π–π electronic interactions in the crystal structures of the two solvates

Ring A	Ring B	Symm. of B	DC /Å	α /deg.	DP1 /Å	DP2 /Å
1×DMF						
3'	4'	2-x,1-y,1-z	3.904	2.01	3.696	3.654
1	4	1-x,-y,1-z	3.673	4.23	3.393	3.398
2'	4	1-x,1/2+y,1/2-z	3.866	23.48	3.836	3.330
4	1	1-x,-y,1-z	3.673	4.23	3.398	3.393
4'	3'	2-x,1-y,1-z	3.904	2.01	3.654	3.696
4'	4'	2-x,1-y,1-z	3.828	0.0	3.659	3.659
1×DMSO						
3	3	2-x,2-y,-z	3.938	0.0	3.712	3.712
3	4	2-x,2-y,-z	4.039	0.64	3.712	3.707
3'	4'	2-x,-y,1-z	3.813	0.42	3.671	3.666
1	4	1-x,1-y,-z	3.709	4.79	3.440	3.410
4	3	2-x,2-y,-z	4.039	0.64	3.707	3.712
4	1	1-x,1-y,-z	3.709	4.79	3.410	3.440
4'	3'	2-x,-y,1-z	3.813	0.42	3.666	3.671

While in **1×DMF** the molecules are connected by π–π electron interactions forming a three-dimensional network, the molecules in **1×DMSO** are linked in such a way that they form layers parallel to the yz plane (see Figure S2). This gives rise to the formation of large cavities in the crystal structure which are filled with THF molecules in a disordered manner.

S3. Competition studies. The response of **1** ($c = 1 \times 10^{-6}$ M) toward other small in/organic anions was tested in the solvent mixture DMSO:water (95:5 vol-%) with the tetrabutylammonium (TBA), tetraethylammonium (TEA) or alkali metal ion salts of various anions, TBA^+F^-, TBA^+Cl^-, TBA^+Br^-, TEA^+I^-, $TBA^+HSO_4^-$, $TBA^+NO_3^-$, TEA^+CN^- (all of them at 20 mM), $Cs^+HCO_3^-$ (0.4 mM), K^+ oxalate (1.4 mM) and Na^+ benzoate (1.0 mM) at the salt concentrations indicated in brackets (whereever $c < 20$ mM, solubility problems hampered an application of a higher excess of anion). No effects were observed for Cl^-, Br^-, I^-, HSO_4^-, NO_3^-, HCO_3^-, oxalate and benzoate, only CN^- led to a slight increase in fluorescence by a factor of 1.2. Only in the case of a high excess of F^-, more pronounced changes where found, conceivable with a deprotonation of the sensor molecule due to the high reactivity of this ion in such kind of solvent mixtures.[2]
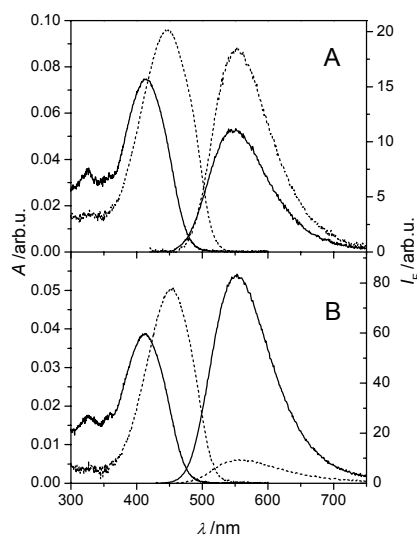

Figure S3 Absorption and fluorescence spectra of (A) **1** and (B) **2** in the absence (–) and presence ($\cdots$) of 20 mM F^- in DMSO:H$_2$O (95:5 vol-%), $c_{dye} = 1 \times 10^{-6}$ M, excitation at the respective isosbestic points

It is interesting to note that the studies with fluoride gave an indirect proof for the photophysical quenching mechanism. At high excess of F^-, only the spectroscopic features of **3** remained unchanged. For **1**, a bathochromic shift of the absorption maximum to 446 nm was noticed, along with an increase in molar absorptivity (Figure S3). At the same time, the fluorescence band position shifted only slightly to longer wavelengths. However, the quantum yield increased by a factor of 1.6 (Figure S3). Concerning **2**, the spectrophotometric changes were almost identical (shift to 454 nm and increase in ε), but for this derivative, the presence of F^- led to fluorescence quenching (Figure S3). Most remarkably, at this high anion concentration, virtually identical fluorescence quantum yields of ca. 0.006 were obtained for **1** and **2** in the presence of F^-. We tentatively assume that the spectroscopic changes can be rationalized in terms of deprotonation of the amido groups of **1** and **2**. Such a reaction would convert A^3 into a strong electron donor, reconfiguring the D^1–A^2–A^3 into a D^1–A^2–D^3 structure, where apparently the D^3–A^2 charge transfer successfully competes with the CT process largely localized on the D^1–A^2 fragment (as in **3**) and induces the bathochromic shifts. In analogy with previous studies,[3] such a CT within the D^3–A^2 fragment most probably involves twisted structures and leads to considerably lower emission yields. Moreover, these results indicate that the amido group in both **2** and **3** is deprived of the hydrogen atom/proton so that the differences in hydrogen bond-assisted quenching are leveled out, resulting in virtually identical fluorescence quantum yields for both dyes.

Protonation on the other hand leads to hypso- and hypochromic shifts for all the three dyes, yielding for instance λ_{abs} = 374 nm (ca. 3 % reduction in ε) for **1**, λ_{abs} = 377 nm (ca. 6 % reduction in ε) for **2** and λ_{abs} = 345 nm (ca. 25 % reduction in ε) for **3** in the presence of 60 mM HClO$_4$. Apparently, attack of the dimethylamino group by protons reduces the CT character, entailing these effects. Furthermore, as has been found by us in previous studies of the bisamidopyridine receptor unit,[4] metal cations do not interfere with the performance of **1** under the present conditions at up to 100 µM (for heavy and transition metal ions) or 20 mM (alkali and alkaline-earth metal ions) concentrations.

In conclusion, the similarity of the fluorescence features of the deprotonated dyes gives further indirect support to our interpretation that not an excited-state chromophoric interaction is responsible for the quenched emission in **1**, but the unique hydrogen bonding properties of this V-shaped compound.

In less polar solvents such as MeCN and CHCl$_3$, the fluorescence amplification effect induced by AcO$^-$ and H$_2$PO$_4^-$ is naturally more pronounced, amounting for instance to a factor of 25 for the former and **1** in MeCN. The other anions listed above show a negligible influence on the emission features, except for F$^-$ and, to a lesser extent, Cl$^-$. Whereas the effect of F$^-$ is conceivable with an even increased tendency to deprotonate the probe, Cl$^-$ shows only a 3.7-fold enhancement of the fluorescence for **1** in MeCN. This behavior strongly suggests that binding of chloride by **1** is less efficient than complexation to the two target anions. Unfortunately, due to the low solubility of **1** in MeCN, NMR studies could not be performed on any pair of **1** and anion. Moreover, in CHCl$_3$ the situation is more complex as **1** obviously exists in two different ground-state species which are well-distinguishable in the absorption spectra. Here, mechanistic investigations are currently being undertaken and we will report on these features at a later stage.

S4. NMR studies. The ^{1}H NMR spectra of **1** in both CDCl$_3$ and DMSO-d$_6$ show only half of the proton signals, thereby demonstrating the symmetry of the molecule. If the integral of the proton H1 is set to 1 (for proton labeling, see Chart S1), the integrals of all other protons are found to be close to 2. The assignment of the signals for **1** and the singly armed model **2** are given in Table S4. In DMSO, the NH signals of both substances appear at lower field as compared to chloroform solution due to N–H···O=S hydrogen bond formation. Moreover, the magnitude of these shifts, $\Delta\delta$ = 1.62 vs. 0.68 for **1** vs. **2**, clearly indicates that the effect is much more pronounced for the sensor molecule, stressing the fact that the unique solid-state features as revealed by the X-ray measurements are generally preserved in solution. Furthermore, in DMSO both protons of the ethenyl group appear as doublets with a coupling constant of ca. 15 Hz, which is characteristic for an E conformation. (The collapse of these signals in CDCl$_3$ resulting in a singlet seems to be accidental and not due to conformational changes.)

The anion binding capability of **1** and **2** in DMSO-d$_6$ was also investigated by ^{1}H NMR spectroscopy. Here, both compounds were titrated with TBA$^+$AcO$^-$. The actual dye-to-anion ratio τ was calculated from the ratio of the integrals of the methyl group signals of both species after every titration step. The changes in the chemical shift of the NH resonances were then monitored as a function of τ. The addition of one equivalent of acetate resulted already in a sizeable downfield shift of the NH protons of **1** ($\Delta\delta \approx$ 0.19 ppm), while the endpoint of $\Delta\delta \approx$ 0.66 ppm is obtained for a 1:4 **1**/AcO$^-$ ratio (Figure S4). This clearly indicates that the bisamidopyridine moiety is able to form a hydrogen bond-assisted complex with acetate ions. The process does not result in a chemical shift differentiation of the side arm protons, pointing to a simultaneous formation of two hydrogen bonds involving both amido hydrogens or fast exchange kinetics. All the other protons experience only negligible shifts, indicating the absence of other strong intermolecular interactions.

In contrast, for **2** the addition of up to four equivalents of AcO$^-$ resulted only in a very small downfield shift of the amido hydrogen, with all the other δ shifts being unaffected (Figure S4).

Apparently, the acetate ions are not able to bind to **2** and replace the DMSO solvent molecule as the hydrogen bond acceptor.
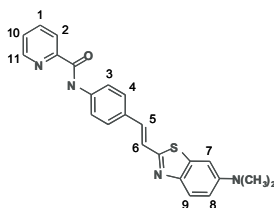

Chart S1 Labeling of the proton positions as used in the NMR section S4

Table S4 Assignments of the ^{1}H NMR signals for **1** and **2** in DMSO-d_6 and CDCl$_3$

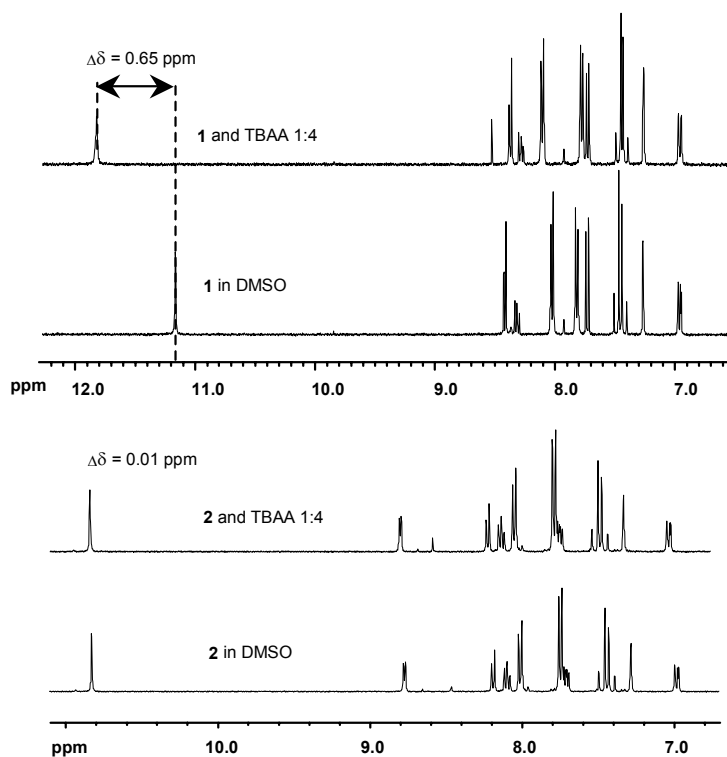| proton	1		2	
	δ /ppm		δ /ppm	
	DMSO-d_6	CDCl$_3$	DMSO-d_6	CDCl$_3$
NH	11.19	9.570	10.823	10.139
1	8.341	8.202	8.092	7.927
2	8.444	8.549	8.183	8.313
3	7.844	7.653	7.740	7.591
4	8.052	7.853	8.006	7.835
5	7.453	7.373	7.412	7.338
6	7.509	7.373	7.460	7.338
7	7.292	7.084	7.280	7.095
8	6.988	6.946	6.979	6.945
9	7.757	7.836	7.740	7.823
10			7.701	7.503
11			8.768	8.633
N(CH$_3$)$_2$	3.004	3.057	2.996	3.047

Figure S4 Changes in the ^{1}H NMR signals of the NH groups of **1** and **2** in the absence and the presence of a 4-fold excess of TBA$^+$AcO$^-$ in DMSO-d_6

References:

1   G. M. Sheldrick, SHELX97, University Göttingen, 1997.
2   C. L. Liotta and H. P. Harris, *J. Am. Chem. Soc.*, 1974, **96**, 2250.
3   K. Rurack, W. Rettig and U. Resch-Genger, *Chem. Commun.*, 2000, 407.
4   J. L. Bricks, G. Reck, K. Rurack, B. Schulz and M. Spieles, *Supramol. Chem.*, 2003, **15**, 189.